Int. J. Heat Mass Transfer. Vol. 31, No. 12, pp. 2505–2516, 1988
Printed in Great Britain

0017–9310/88 $3.00 + 0.00

Mixed convection boundary layer flow on a horizontal plate in a uniform stream

TASAWWUR HUSSAIN
K.D.M. Institute of Petroleum Exploration, Dehradun 248195, India

and

NOOR AFZAL
Department of Mechanical Engineering, Aligarh Muslim University, Aligarh 202001, India

(*Received* 25 *March* 1986 *and in final form* 6 *November* 1986)

Abstract—A mixed convection boundary layer on a horizontal plate for uniform wall temperature/uniform heat flux is investigated using a computer extension of the perturbation series. The first 17 terms for the uniform wall temperature case and the first ten terms for the uniform heat flux case are computed for a Prandtl number $\sigma = 0.72$. The direct expansion is transformed by a Euler transform and other techniques. The results for buoyancy aiding or opposing the main flow are presented. The present work predicts the result to two digit accuracy for the entire domain of the streamwise coordinate. For uniform wall temperature, the maximum error is 5.983% for skin friction and 1.072% for heat transfer. For uniform heat flux, the maximum error is 6.9% for skin friction and 1.9% for wall temperature.

1. INTRODUCTION

IN THE mixed convection on a horizontal plate, the tangential component of buoyancy gives rise to a hydrostatic pressure distribution across the boundary layer which modifies the forced convection boundary layer. As the boundary layer develops, the hydrostatic pressure at the plate surface also increases with increasing distance from the leading edge. The buoyancy force can either aid or oppose the development of the forced convection boundary layer depending on whether the induced pressure gradient within the boundary layer is favourable or adverse. More specifically, for an upward facing heated horizontal plate the density near the plate is less than the ambient density, the hydrostatic pressure at the surface decreases as the distance increases from the leading edge giving rise to a negative pressure gradient which accelerates the flow that results in the aiding flow situation. Likewise, above a cool horizontal plate there is an adverse pressure gradient. As the adverse pressure gradient is due to buoyancy, this results in an opposing flow situation. In the later situation if the buoyancy effects are stronger, the opposition of the forced and free convection effects leads to separation of the flow. The characteristics of a mixed convection boundary layer depends on the velocity of the forced stream and the thermal conditions at the wall, which later can be either a prescribed wall temperature or prescribed heat flux at the wall.

The mixed convection on the horizontal surface due to a uniform oncoming stream has been studied by many workers. For buoyancy aiding flows, the results are well documented but in opposing flow situations, the investigations are largely incomplete. Mori [1] considered the weakly buoyant flows by expanding the variables in terms of a direct coordinate expansion valid in a region near the leading edge of the plate. The numerical solutions for the first-order perturbations were reported for a Prandtl number of $\sigma = 0.72$. Sparrow and Minkowycz [2] have corrected a minor sign error in the analysis of ref. [1] and presented numerical solutions for Prandtl numbers, $\sigma = 0.01$, 0.7 and 10. A perturbation series in terms of the distance from the leading edge apply as such to small buoyancy effects [2–5]. Further, Hieber [5] also studied the strongly buoyant flows in terms of an inverse coordinate expansion and the solutions to the first three terms in the inverse expansion were reported for a Prandtl number of $\sigma = 0.72$. The two expansions, direct and inverse, do not describe the entire mixed convection domain and fail in a domain where mixed convection effects are moderate. For limiting Prandtl numbers, the solutions of the equations for direct and inverse coordinate expansions were reported by Hieber [5] and Leal [6]. Approximate solutions of the modified boundary layer equations were obtained by Martynenko and Sokovishin [7] using an integral method similar to that of Karman–Pohlhausen. Chen *et al.* [8] and Mucoglu and Chen [9] have studied the problem by local similarity and related methods. Experimental results were reported by Wang [10]. The numerical solutions were reported by Ramachandran *et al.* [11]. Also, a vortex instability of the fluid flow heated from below or cooled from above was studied by Wang [10] and Moutsoglou *et al.* [12]. Reference [13] considered the Navier–Stokes equations by employing the method of series truncation. The

numerical solutions to first truncated equations have been reported for various Reynolds and Grashof numbers.

The mixed convection problem for a prescribed heat flux at the wall has been studied by Mucoglu and Chen [9] and Schneider and Wasel [14]. The free convection asymptote has been studied in ref. [15] by employing boundary conditions at the wall implicitly and in ref. [16] explicitly. In particular self-similar solutions have been studied by Schneider [17] for a wall temperature prescribed as an inverse square root of the distance from the leading edge.

Recently, Raju *et al.* [18] and Schneider and Wasel [14] have studied the mixed convection on a horizontal plate by integrating the boundary layer equations by finite difference schemes. The cases of prescribed wall temperature and prescribed heat flux are considered. Raju *et al.* [18] presented a formulation (see also ref. [19]) where the entire mixed convection domain has been studied through a single formulation resulting in the smooth transition from one convection limit to the other. They provided the solutions in the aiding and opposing flow situations. For the opposing flow situation velocity and temperature profiles are displayed graphically but shear stress and heat transfer distribution along the plate are not given. Schneider and Wasel [14] describe the solutions in the adverse flow domain where streamwise gradient and heat transfer approach infinity. They attribute this infinite behaviour to the failure of the boundary layer equations. In a related problem of similar solutions for mixed convection on a horizontal plate ref. [20] has shown that the solutions are dual with a turning point where the shear stress is still finite. This conclusion was also supported from the solutions of de Hoog *et al.* [21] and the work of Raju *et al.* [18].

The present work deals with the extension of a direct series to estimate several higher order terms for the two cases of prescribed uniform wall temperature and uniform heat flux at the wall. The first 17 terms for the uniform wall temperature case and ten terms for the uniform heat flux case have been obtained. It is shown that the results of the direct series expansions when transformed by the Euler transformation and other techniques predict results correct to two decimal places even in the asymptotic case of strongly buoyant flows.

2. EQUATIONS OF MOTION

The boundary layer equations for mixed convection flow over a horizontal semi-infinite flat plate under the Boussinesq approximation representing conservation of mass, momentum and energy are

$$\frac{\partial u}{\partial x}+\frac{\partial v}{\partial y}=0 \tag{1}$$

$$u\frac{\partial u}{\partial x}+v\frac{\partial u}{\partial y}=-\frac{1}{\rho}\frac{\partial p}{\partial x}+\nu\frac{\partial^2 u}{\partial y^2} \tag{2}$$

$$\frac{1}{\rho}\frac{\partial p}{\partial y}=\pm g\beta(T-T_\infty) \tag{3}$$

$$u\frac{\partial T}{\partial x}+v\frac{\partial T}{\partial y}=\frac{\nu}{\sigma}\frac{\partial^2 T}{\partial y^2}. \tag{4}$$

The boundary conditions are

$$u=0,\quad T=T_w(x)\quad\text{or}\quad \frac{\partial T}{\partial y}=-\frac{q}{k}\quad\text{at}\quad y=0 \tag{5a,b}$$

$$u\to U_\infty,\quad T\to T_\infty\quad\text{as}\quad y\to\infty. \tag{5c}$$

Here x is the coordinate along the plate measured from the leading edge and y normal to it. u and v are velocity components in the x- and y-directions, respectively. U_∞ is the constant uniform velocity of the free stream and T_∞ the temperature of the free stream. An integration of energy equation (4) over a large control volume enclosing the leading edge gives the total heat flux Q as

$$Q=\rho C_p\int_0^\infty u(T-T_\infty)\,dy. \tag{6}$$

3. ANALYSIS

3.1. *Uniform wall temperature case*

In the region near the leading edge of the plate, the boundary layer is mainly governed by forced convection flow and the buoyancy effects can be regarded as perturbations. The appropriate variables are therefore Blasius variables defined by

$$\psi=(\nu U_\infty x)^{1/2}f(\xi,\eta),\quad T-T_\infty=\Delta T\theta(\xi,\eta),$$
$$p=\rho U^2 G(\xi,\eta),\qquad \Delta T=T_w-T_\infty. \tag{7}$$

The variables ξ and η are defined by

$$\xi=Gr_x/Re_x^{5/2},\quad \eta=y\left(\frac{U_\infty}{\nu x}\right)^{1/2} \tag{8a}$$

where Gr_x and Re_x are local Grashof and Reynolds number, respectively, defined by

$$Gr_x=\frac{g\beta(T_w-T_\infty)x^3}{\nu^2},\quad Re_x=\frac{U_\infty x}{\nu}. \tag{8b}$$

The stream function, ψ, is defined as

$$u=\frac{\partial\psi}{\partial y}\quad\text{and}\quad v=-\frac{\partial\psi}{\partial x}. \tag{9}$$

Substituting transformations (7)–(9) into boundary layer equations (1)–(4) we obtain the following non-similar equations:

$$f'''+\tfrac{1}{2}ff''+\tfrac{1}{2}\eta G'=\tfrac{1}{2}\xi(f'f'_\xi-f_\xi f''+G_\xi) \tag{10}$$

$$G'=\pm\xi\theta \tag{11}$$

$$\frac{1}{\sigma}\theta''+\tfrac{1}{2}f\theta=\tfrac{1}{2}\xi(f'\theta_\xi-f_\xi\theta'). \tag{12}$$

Boundary conditions (5a) and (5c) become

$$f(\xi,0) = f'(\xi,0) = \theta(\xi,0) - 1 = 0 \quad (13a)$$

$$f'(\xi,\infty) - 1 = \theta(\xi,\infty) = 0. \quad (13b)$$

The global heat flux condition (6) gives

$$Q = (\rho C_p \Delta T \sqrt{(\nu U_\infty x)}) \int_0^\infty f'\theta \, d\eta. \quad (14)$$

The positive and negative sign with the buoyancy term in equation (11) represents buoyancy aiding and opposing the main flow.

For weakly buoyant flows, ξ is small and the variables can be expanded in power series as

$$f(\xi,\eta) = \sum_{n=0}^{\infty} (\pm\xi)^n f_n(\eta)$$

$$G(\xi,\eta) = \sum_{n=0}^{\infty} (\pm\xi)^n G_n(\eta)$$

$$\theta(\xi,\eta) = \sum_{n=0}^{\infty} (\pm\xi)^n \theta_n(\eta). \quad (15a\text{–}c)$$

Substituting expansions (15) in equations (10)–(12) and equating various powers of ξ we obtain the equations for successive approximations. The equations for leading order ($n = 0$) are

$$f_0''' + \tfrac{1}{2} f_0 f_0'' = 0, \quad G_0' = 0 \quad (16a,b)$$

$$\frac{1}{\sigma}\theta_0'' + \tfrac{1}{2} f_0 \theta_0' = 0 \quad (17)$$

$$f_0(0) = f_0'(0) = \theta_0(0) - 1 = f_0'(\infty) - 1 = \theta_0(\infty) = 0. \quad (18)$$

Global heat flux condition (14) gives

$$Q = (\rho C_p \Delta T \sqrt{(\nu U_\infty x)}) \int_0^\infty f_0' \theta_0 \, d\eta. \quad (19)$$

Equations (16) and (17) are not coupled and the momentum equation is the well-known Blasius equation. The equations for the next highest order perturbation (f_n, θ_n) for $n > 1$ can be expressed in terms of recurrence relations as

$$f_n''' + \tfrac{1}{2} f_0 f_n'' - \tfrac{1}{2} n f_0 f_n' + \frac{(n+1)}{2} f_0'' f_n + \tfrac{1}{2}\eta\theta_{n-1} - \frac{n}{2} G_n = \frac{1}{2}\sum_{r=1}^{n-1} [r f_{n-r}' f_r' - (r+1) f_r f_{n-r}''] \quad (20)$$

$$G_n' = \theta_{n-1} \quad (21)$$

$$\frac{1}{\sigma}\theta_n'' + \tfrac{1}{2} f_0 \theta_n' - \tfrac{1}{2} n f_0' \theta_n + \frac{(n+1)}{2} f_n \theta_0' = \frac{1}{2}\sum_{r=1}^{n-1} [r f_{n-r}' \theta_r - (r+1) f_r \theta_{n-r}']. \quad (22)$$

The boundary conditions for $n > 1$ are

$$f_n(0) = f_n'(0) = \theta_n(0) = f_n'(\infty) = \theta_n(\infty) = 0 \quad (23)$$

and integral heat flux condition for $n > 1$ is

$$\int_0^\infty \left(f_n'\theta_0 + f_0'\theta_n + \sum_{r=1}^{n-1} f_r'\theta_{n-r} \right) d\eta = 0. \quad (24)$$

Equations (21) and (22) are decoupled by virtue of equation (21) and can be solved successively.

3.2. *Uniform heat flux case*

In this case, the appropriate similarity transformations in terms of forced convection variables are defined by

$$\psi = (\nu U_\infty x)^{1/2} f(\hat{\xi},\eta), \quad T - T_\infty = \frac{q}{k}\left(\frac{\nu x}{U_\infty}\right)^{1/2} \theta(\hat{\xi},\eta) \quad (25)$$

$$p = \rho U^2 G(\xi,\eta), \quad \eta = y\left(\frac{U_\infty}{\nu x}\right)^{1/2} \quad (26)$$

where

$$\hat{\xi} = \left(\frac{\nu g \beta q}{k U_\infty^3}\right) x. \quad (27)$$

Based on equations (25)–(27), boundary layer equations (1)–(4) become

$$f''' + \tfrac{1}{2} f f'' + \tfrac{1}{2}\eta G' = \hat{\xi}(f_{\hat{\xi}} f' - f_{\hat{\xi}} f'' + G_{\hat{\xi}}) \quad (28)$$

$$G' = \pm\hat{\xi}\theta \quad (29)$$

$$\frac{1}{\sigma}\theta'' + \tfrac{1}{2} f\theta' - \tfrac{1}{2} f'\theta = \hat{\xi}(f'\theta_{\hat{\xi}} - f_{\hat{\xi}}\theta'). \quad (30)$$

The boundary conditions are

$$f(\hat{\xi},0) = f'(\hat{\xi},0) = \theta'(\xi,0) + 1 = 0,$$

$$f'(\hat{\xi},\infty) - 1 = \theta(\hat{\xi},\infty) = 0 \quad (31a,b)$$

subject to the integral heat flux condition

$$Q = \left(\frac{\rho C_p \nu q}{k} x\right) \int_0^\infty f'\theta \, d\eta. \quad (32)$$

The positive and negative sign in equation (29) is indicative of buoyancy aiding and opposing flow situations.

For weakly buoyant flows, $\hat{\xi}$ is small and the variables in equations (28)–(30) can be expanded in powers of $\hat{\xi}$ in a manner similar to equations (15) and substituting these expansions into equations (28)–(30) and equating various powers of $\hat{\xi}$, we obtain the equations for successive approximations. The equations for the leading order ($n = 0$) approximations for momentum and pressure are the same as equations (16a) and (16b) and the energy equation is given by

$$\frac{1}{\sigma}\theta_0'' + \tfrac{1}{2} f_0 \theta_0' - \tfrac{1}{2} f_0' \theta_0 = 0 \quad (33)$$

$$f_0(0) = f_0'(0) = \theta_0'(0) + 1 = 0,$$

$$f_0'(\infty) - 1 = \theta_0(\infty) = 0. \quad (34a,b)$$

Global heat flux condition (32) gives

$$Q = \left(\frac{\rho C_p \nu q}{k} x\right) \int_0^\infty f_0' \theta_0 \, d\eta. \tag{35}$$

The higher order approximations for $n > 1$ are expressed by recursive relations as

$$f_n''' + \tfrac{1}{2} f_0 f_n'' - n f_0' f_n' + (n + \tfrac{1}{2}) f_0'' f_n + \tfrac{1}{2} \eta \theta_{n-1} - n G_n = \sum_{r=1}^{n-1} [r f_{n-r}' f_r' - (r + \tfrac{1}{2}) f_r f_{n-r}''] \tag{36}$$

$$G_n' = \theta_{n-1} \tag{37}$$

$$\frac{1}{\sigma} \theta_n'' + \tfrac{1}{2} f_0 \theta_n' - (n + \tfrac{1}{2}) f_0' \theta_n + (n + \tfrac{1}{2}) \theta_0' f_n - \tfrac{1}{2} f_n' \theta_0 = \sum_{r=1}^{n-1} [(r + \tfrac{1}{2})(f_{n-r}' \theta_r - f_r \theta_{n-r}')]. \tag{38}$$

The boundary conditions for $n > 1$ are

$$f_n(0) = f_n'(0) = \theta_n'(0) = f_n'(\infty) = \theta_n(\infty) = 0 \tag{39}$$

and the integral heat flux condition for $n > 1$ is the same as that given by equation (24).

4. RESULTS AND DISCUSSIONS

The calculations of higher order perturbation approximations in recurrence relations (20)–(24) for small ξ and equations (36)–(39) together with the integral heat flux condition for small ξ are programmed as nested 'DO' loops.

4.1. *Uniform wall temperature case*

The results for skin friction and heat transfer rate are given by

$$f''(\xi, 0) = \sum_{n=0}^{16} a_n (\pm \xi)^n \tag{40a}$$

$$\theta'(\xi, 0) = \sum_{n=0}^{16} b_n (\pm \xi)^n \tag{40b}$$

where the coefficients a_n, b_n are given in Table 1.

The positive and negative sign with ξ corresponds to favourable and adverse buoyancy with respect to the oncoming stream. Figure 1 displays Domb–Sykes [22] plots, i.e. ratios a_n/a_{n-1} or b_n/b_{n-1} against $1/n$. The extrapolation to $1/n = 0$ yields an estimate of the radius of convergence $|\xi_0|$. The Domb–Sykes plots of series (40) shown in Fig. 1 do not appear to have settled down and it is not easy to extrapolate the points to get the radius of convergence. However, the turning point studied earlier can be regarded as representative of the nearest singularity. We adopt $\xi_0 = 0.057$, as it is well known that a slight variation in the value of ξ_0 does not affect much the results of the Euler transformation (see Appendix A of ref. [27]).

For buoyancy aiding flow situations, the nearest singularity on the negative real axis in the complex ξ-plane, at $\xi = -\xi_0$ can be mapped away to infinity by the Euler transformation

$$Z = \frac{\xi}{\xi + \xi_0} \tag{41}$$

where ξ_0 is the radius of convergence.

As $\xi \to \infty$, $f''(\xi, 0) \sim \xi^{3/5}$ and $\theta'(\xi, 0) \sim \xi^{1/5}$, extracting the factors $\xi^{3/5}$ and $\xi^{1/5}$ from series (40a) and (40b), respectively, and recasting the series in terms of variable Z defined by equation (41), we have

$$\xi^{-3/5} f''(\xi, 0) = \sum_{n=0}^{16} A_n Z^{n-3/5} \tag{42a}$$

$$\xi^{-1/5} \theta'(\xi, 0) = \sum_{n=0}^{16} B_n Z^{n-1/5}. \tag{42b}$$

Coefficients A_n and B_n of the transformed series (42) are given in Table 1. Series (42) are hopefully con-

Table 1. Coefficients in the series for skin friction and heat transfer for mixed convection on a horizontal plate with uniform wall temperature: a_n, b_n, low ξ series (40): A_n, B_n, Eulerized series (42)

	Skin friction		Heat transfer	
n	a_n	A_n	b_n	B_n
0	0.332057357E+00	0.185220146E+01	−0.295635290E+00	−0.524301752E+00
1	0.169711945E+01	−0.571732799E+00	−0.355730463E+00	0.689002473E−01
2	−0.499843675E+01	−0.970145064E−01	0.158582043E+01	0.223135857E−01
3	0.357306689E+02	−0.425486865E−01	−0.122196806E+02	0.117093884E−01
4	−0.337330268E+03	−0.248289643E−01	0.118215763E+03	0.745357242E−02
5	0.368597704E+04	−0.166257151E−01	−0.130260244E+04	0.526725798E−02
6	−0.442052844E+05	−0.120742679E−01	0.156493787E+05	0.397409451E−02
7	0.566285662E+06	−0.925165160E−02	−0.200199785E+06	0.313579508E−02
8	−0.762691768E+07	−0.736427483E−02	0.268838190E+07	0.255622241E−02
9	0.106889482E+09	−0.603235263E−02	−0.375359582E+08	0.213600297E−02
10	−0.154752459E+10	−0.505414832E−02	0.541229348E+09	0.182003704E−02
11	0.230446382E+11	−0.431090527E−02	−0.802455605E+10	0.157535368E−02
12	−0.351496882E+12	−0.371820982E−02	0.121867303E+12	0.138020602E−02
13	0.547711842E+13	−0.319018255E−02	−0.189076999E+13	0.121736515E−02
14	−0.869853463E+14	−0.260041362E−02	0.299018215E+14	0.106843086E−02
15	0.140552127E+16	−0.172830028E−02	−0.481154558E+15	0.907266502E−03
16	−0.230726465E+17	−0.179503953E−03	0.786715016E+16	0.691037964E−03

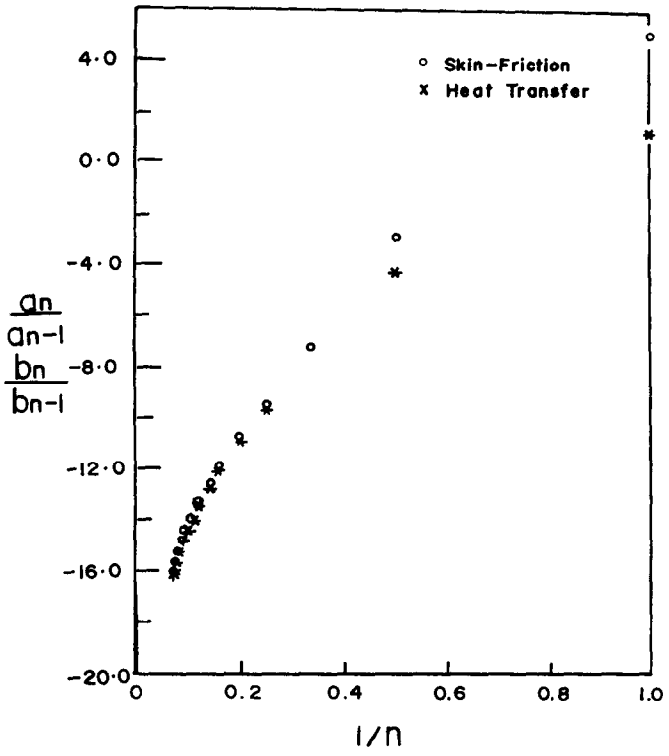

FIG. 1. The Domb–Sykes plots for skin friction and heat transfer series (45) for mixed convection on a horizontal flat plate with constant wall temperature: ○, skin friction; *, heat transfer.

vergent for all values of Z from $Z = 0$ to 1, provided there is no other singularity. The last partial sums of series (42) at $Z = 1$ yield the value for skin friction, $\xi^{-3/5} f''(\xi, 0) = 1.043946$, and for heat transfer rate at the wall, $\xi^{-1/5}\theta'(\xi, 0) = -0.388196$, whereas the corresponding exact results of Rotem and Classen [23] and Hieber [5] obtained from the study of strongly buoyant flows ($\xi \to \infty$) for skin friction and heat transfer, respectively, are 0.97840 and −0.35741. This shows that the last partial sums of transformed series (42) overestimate the skin friction by 6.69% and heat transfer by 8.61%.

The convergence of transformed series (42) can further be improved by completing series (42) from the analysis of the remainder. The remainder can be adopted from the characteristics of the Domb–Sykes plots: the inverse ratios A_n/A_{n-1} or B_n/B_{n-1} against $1/n$, displayed in Fig. 2. A line with slope 2/5 and

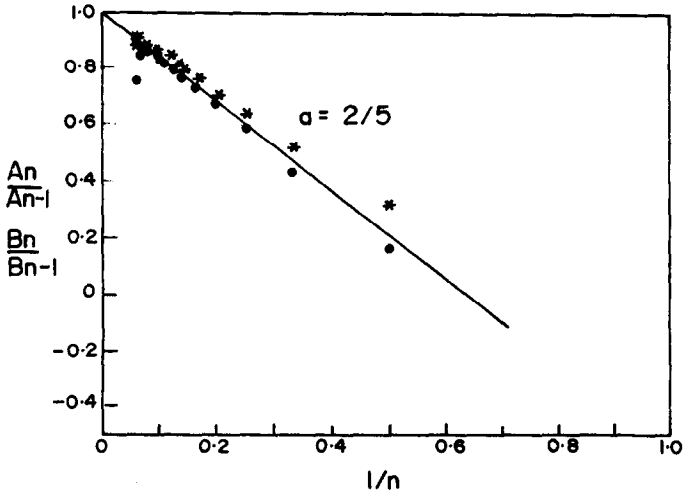

FIG. 2. The Domb–Sykes plots for Eulerized series (48) for skin friction and heat transfer for mixed convection on a horizontal plate with constant wall temperature: ●, skin friction; *, heat transfer.

Table 2. Coefficients in the series for skin friction and heat transfer for mixed convection on a horizontal plate with uniform wall temperature: A_n, B_n, completed Eulerized series (43)

n	Skin friction A_n^*	Heat transfer B_n^*
−1	0.318410446E−01	−0.122578752E+00
0	0.182036041E+01	−0.401722999E+00
1	−0.558996381E+00	0.198687454E−01
2	−0.931935810E−01	0.760413530E−02
3	−0.405108596E−01	0.386434821E−02
4	−0.235043768E−01	0.235429631E−02
5	−0.156720121E−01	0.159577918E−02
6	−0.113430956E−01	0.115929410E−02
7	−0.866671378E−02	0.883954760E−03
8	−0.688170113E−02	0.698454148E−03
9	−0.562484595E−02	0.567220883E−03
10	−0.470369257E−02	0.470884446E−03
11	−0.400505298E−02	0.397911417E−03
12	−0.344804030E−02	0.340132021E−03
13	−0.294910821E−02	0.289299121E−03
14	−0.238344671E−02	0.233171434E−03
15	−0.153158361E−02	0.149964623E−03

intercept unity is also displayed in the same figure. The figure shows that the line is in agreement except for a few points for large n. Therefore, the remainder can be taken proportional to $(1-Z)^{2/5}$ and the constant of proportionality is determined by equating the 17 terms. On completing, the transformed series (42) leads to

$$\xi^{-3/5} f''(\xi,0) = Z^{-3/5}\left[A^*_{-1}(1-Z)^{2/5} + \sum_{n=0}^{15} A_n^* Z^n\right] \tag{43a}$$

$$\xi^{-1/5}\theta'(\xi,0) = Z^{-1/5}\left[B^*_{-1}(1-Z)^{2/5} + \sum_{n=0}^{15} B_n^* Z^n\right]. \tag{43b}$$

Coefficients A_n^* and B_n^* of the completed transformed series (43) are given in Table 2, which are much reduced in comparison to the original coefficients A_n and B_n of transformed series (42). The last partial sums of the completed transformed series (43) for $Z = 1$ yield the value of the skin friction and heat transfer at the wall as $\xi^{-3/5} f''(\xi,0) = 1.03694$ and $\xi^{-1/5}\theta'(\xi,0) = -0.361245$. When compared to exact results, this shows that the results obtained from the completed transformed series (43) at $Z = 1$ ($\xi \to \infty$) underestimate the skin friction by 5.98% and heat transfer at the wall by 1.07%.

The results for skin friction and heat transfer at the wall based on the completed transformed series (43) are displayed in Figs. 3 and 4 against ξ. The asymptotes for small and large ξ are also displayed in the respective figures. Figures 3 and 4 show that the large ξ asymptote for skin friction is reliable when $\xi > 100$ and for heat transfer when $\xi > 1000$.

When the buoyancy opposes the main stream, series (40) are of limited interest. As the nature and location

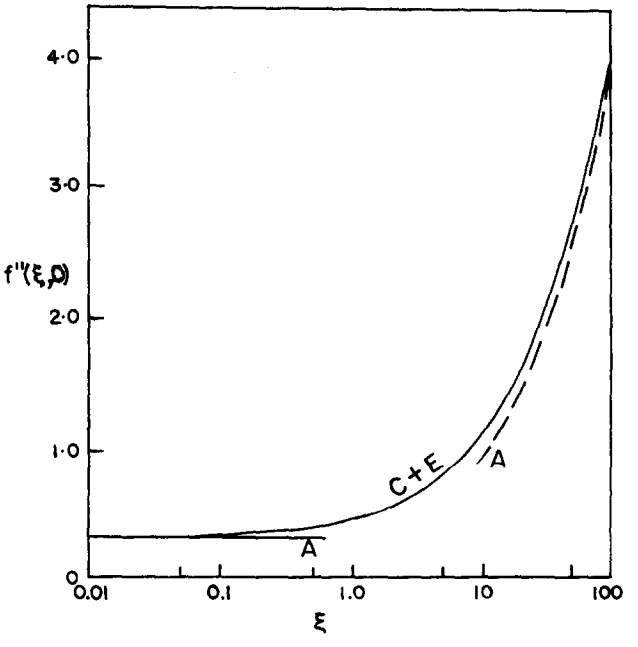

FIG. 3. Favourable case: the comparison of skin friction for mixed convection on a horizontal flat plate with constant wall temperature: C+E, completed transformed series (49a); A, asymptotes for small and large values of ξ.

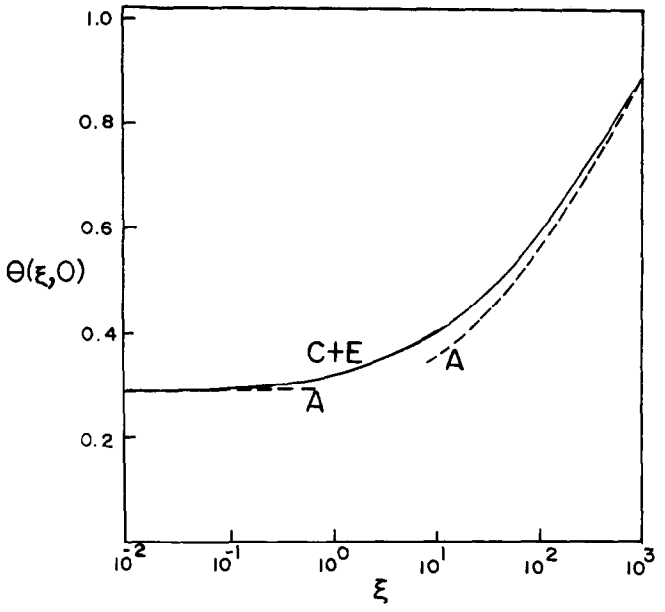

FIG. 4. Favourable case: the comparison of heat transfer for mixed convection on a horizontal flat plate with constant wall temperature: C+E, completed transformed series (49b); A, asymptotes for small and large values of ξ.

of the nearest singularity is not known, it is not possible to improve the series by the method of subtraction of singularities. Guided by the earlier works on the subject [20, 21], dual solutions are expected. A good insight into the structure of the dual solutions can hopefully be gained by inverting series (40) [24]. The method of inverting the series is described as follows.

For a given series

$$y = x^{\lambda+1} \sum_{n=0}^{\infty} \alpha_n x^n \tag{44}$$

its inversion is given by

$$x = \sum_{m=0}^{\infty} \frac{\beta_m}{m+1} y^{-\mu}, \quad \mu = -\left(\frac{m+1}{\lambda+1}\right) \tag{45}$$

where coefficients β_m are given by [26]

$$\beta_0 = \alpha_0^{\mu}, \quad \beta_m = \frac{1}{m\alpha_0} \sum_{n=1}^{m} (n\mu - m + n)\alpha_n \beta_{m-n}. \tag{46}$$

Using the above, series (40) yields

$$\xi(f'') = \sum_{n=1}^{16} c_n \left(\frac{f''-a_0}{a_1}\right)^n \tag{47a}$$

$$\xi(\theta') = \sum_{n=1}^{16} d_n \left(\frac{\theta'-b_0}{b_1}\right)^n \tag{47b}$$

where $f'' = f''(\xi, 0), \theta' = \theta'(\xi, 0)$ and the coefficients c_n and d_n are given in Table 3. The results for skin friction and heat transfer are displayed against ξ, the mixed convection parameter in Fig. 5 show the dual solutions and associated turning point. The skin friction and heat transfer decrease with increasing ξ until the turning point is approached. The results for skin friction show that the turning point is around $\xi_0 = 0.057$ whereas those for heat transfer show a slightly smaller value. The slight difference in the location of the turning point is due to different rates of convergence of the two series. Better solutions around the turning point can be obtained from an asymptotic analysis in the neighbourhood of the turning point or from solutions of full partial differential

Table 3. Coefficients in the inverted series (47) for skin friction and heat transfer for mixed convection on a horizontal plate with uniform wall temperature

n	Skin friction c_n	Heat transfer d_n
1	0.100000000E+01	0.100000000E+01
2	0.294524746E+01	0.445792699E+01
3	−0.370474957E+01	0.539527244E+01
4	0.164668560E+02	0.961257557E+01
5	−0.111407057E+03	−0.397975081E+02
6	0.933215908E+03	0.335705186E+03
7	−0.889355797E+04	−0.303887731E+04
8	0.926672385E+05	0.297345384E+05
9	−0.102028465E+07	−0.293451594E+06
10	0.116396648E+08	0.297271786E+07
11	−0.150803586E+09	−0.493052408E+08
12	0.174232427E+10	0.149958878E+09
13	−0.243618618E+11	−0.914492188E+10
14	0.306394790E+12	0.998754352E+10
15	−0.432396958E+13	−0.128509069E+13
16	0.592994893E+14	0.834867382E+13

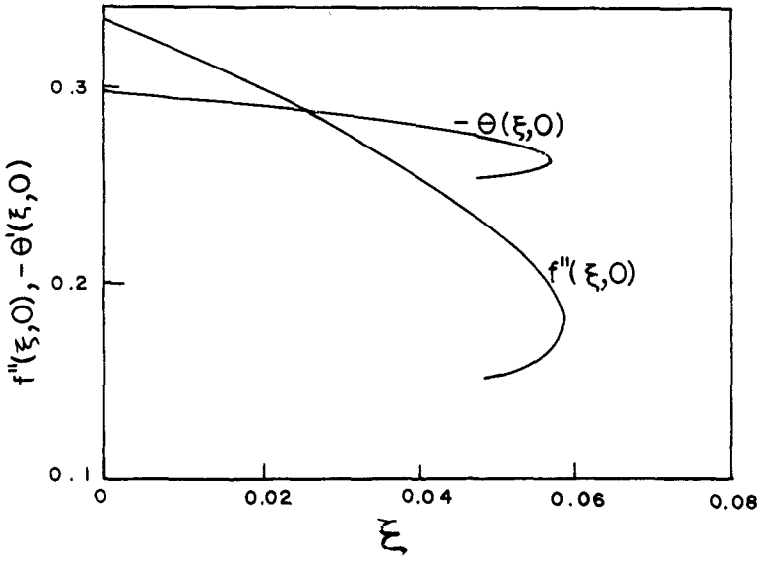

FIG. 5. Adverse case: the characteristics of mixed convection on a horizontal flat plate with constant wall temperature: $f''(\xi,0)$, skin friction; $\theta'(\xi,0)$, heat transfer rate.

equations. The realization of the lower branch solution follows similar arguments as found in ref. [20].

4.2. *Uniform heat flux case*

The results for skin friction and wall temperature are

$$f''(\hat{\xi},0) = \sum_{n=0}^{9} a_n(\pm\hat{\xi})^n \tag{48a}$$

$$\theta(\hat{\xi},0) = \sum_{n=0}^{9} b_n(\pm\hat{\xi})^n. \tag{48b}$$

Coefficients a_n and b_n are given in Table 4. The Domb–Sykes plots a_n/a_{n-1} or b_n/b_{n-1} against $1/n$ are shown in Fig. 6. The extrapolation to $1/n = 0$ leads to an intercept of 50 and a slope of $a = 1$. The reciprocal of the intercept gives the radius of convergence $\hat{\xi}_0 = 0.02$.

To improve the convergence of series (48) for a favourable case the series is recast in terms of the Euler variable defined by equation (41)

$$\hat{\xi}^{-1/2} f''(\hat{\xi},0) = \sum_{n=0}^{9} A_n Z^{n-1/2} \tag{49a}$$

$$\hat{\xi}^{1/6}\theta(\hat{\xi},0) = \sum_{n=0}^{9} B_n Z^{n+1/6}. \tag{49b}$$

Coefficients A_n and B_n are given in Table 4. Series (49a) and (49b) are hopefully convergent for $Z \to 1$ ($\hat{\xi} \to \infty$), provided there is no other singularity. The last partial sums of series (49) yield the value of skin friction, $\hat{\xi}^{-1/2} f''(\hat{\xi},0) = 1.57159897$ and wall temperature $\hat{\xi}^{1/6}\theta(\hat{\xi},0) = 1.65679325$, whereas the pure free convection asymptotes studied in ref. [16] are $f''(0) = 1.52664$ and $\theta(0) = 1.90551$.

The last partial sums of transformed series (49) overestimate the skin friction by 2.945% and underestimate the temperature at the wall by 13.0% approximately.

Table 4. Coefficients in the series for skin friction and wall temperature for mixed convection on a horizontal plate with uniform heat flux: a_n, b_n, low $\hat{\xi}$ series (48): A_n, B_n, Eulerized series (49)

	Skin friction		Wall temperature	
n	a_n	A_n	b_n	B_n
0	0.332057357E+00	0.234800009E+01	0.243978834E+01	0.127113148E+01
1	0.442016066E+01	−0.548894928E+00	−0.551946354E+01	0.154342363E+00
2	−0.440842429E+02	−0.105636522E+00	0.795963325E+02	0.730717581E−01
3	0.952863646E+03	−0.454670821E−01	−0.176440796E+04	0.451503156E−01
4	−0.268694008E+05	−0.258093958E−01	0.482950524E+05	0.315747788E−01
5	0.874048752E+06	−0.168314969E−01	−0.150434767E+07	0.237432708E−01
6	−0.311838521E+08	−0.119450592E−01	0.512430622E+08	0.187314748E−01
7	0.118785028E+10	−0.898301044E−02	−0.186519388E+10	0.152914158E−01
8	−0.475750523E+11	−0.706259901E−02	0.715184452E+11	0.128084067E−01
9	0.198329148E+13	−0.577103815E−02	−0.286090506E+13	0.109479986E−01

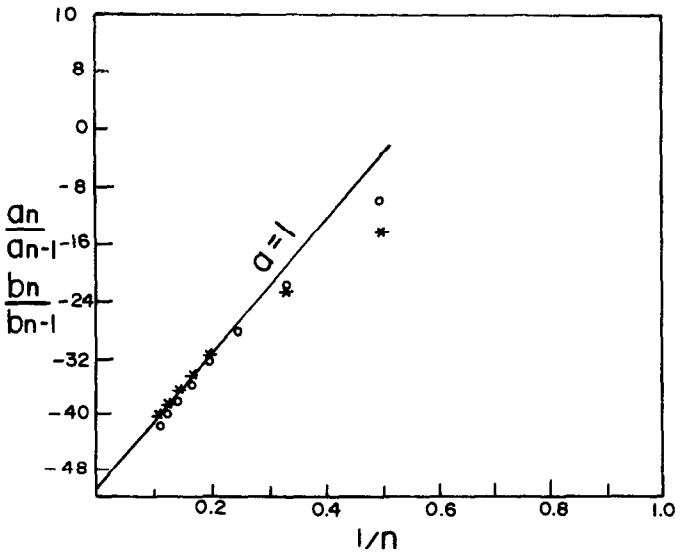

FIG. 6. The Domb–Sykes plots for skin friction and wall temperature series (56) for mixed convection on a horizontal plate with constant heat flux: ○, skin friction; *, temperature.

The convergence of series (49) can hopefully be further improved by completing series (49) from the analysis of the remainder. The Domb–Sykes plots of the inverse ratios A_n/A_{n-1} or B_n/B_{n-1} against $1/n$ on extrapolation to $1/n = 0$ gives the radius of convergence as unity and the slope as $a = 1/3$. The method of subtraction of singularity leads to

$$\hat{\xi}^{-1/2} f''(\hat{\xi}, 0) = Z^{-1/2}\left[A^*_{-1}(1-Z)^{1/3} + \sum_{n=0}^{8} A_n^* Z^n\right] \tag{50a}$$

$$\hat{\xi}^{1/6}\theta(\hat{\xi}, 0) = Z^{1/6}\left[B^*_{-1}(1-Z)^{1/3} + \sum_{n=0}^{8} B_n^* Z^n\right]. \tag{50b}$$

Coefficients A_n^* and B_n^* are given in Table 5. The last partial sums of the transformed–completed series (50) at $Z = 1$ yield the value of skin friction, $\hat{\xi}^{-1/2} f''(\hat{\xi}, 0) = 1.421552$, and wall temperature, $\hat{\xi}^{1/6}\theta(\hat{\xi}, 0) = 1.941441$, showing that the result predicted from series (50) as $\hat{\xi} \to \infty$ underestimate the skin friction by 6.9% and overestimate the tem-

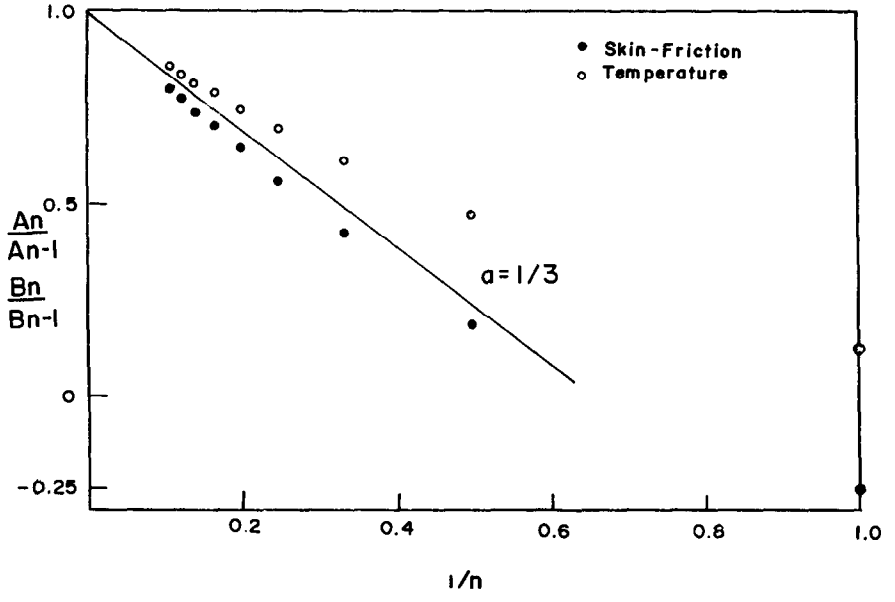

FIG. 7. The Domb–Sykes plots of Eulerized series (58) for skin friction and temperature for mixed convection on a horizontal flat plate with constant heat flux.

Table 5. Coefficients in the series for skin friction and wall temperature for mixed convection on a horizontal plate with uniform heat flux: A_n, B_n, completed Eulerized series (50)

n	Skin friction A_n^*	Wall temperature B_n^*
−1	0.427849286E+00	−0.811655245E+00
0	0.192015080E+01	0.208278672E+01
1	−0.406278495E+00	−0.116209393E+00
2	−0.580977117E−01	−0.171121593E−01
3	−0.190566321E−01	−0.495186046E−02
4	−0.820242920E−02	−0.182667178E−02
5	−0.391972143E−02	−0.751126231E−03
6	−0.190256719E−02	−0.319722850E−03
7	−0.853374066E−03	−0.130982270E−03
8	−0.287902042E−03	−0.435916731E−04

perature at the wall by 1.9%. The relatively large error in skin friction results may be due to the limited number of terms (ten terms) considered. The results for skin friction and temperature at the wall based on the completed–transformed series (50) are displayed in Figs. 8 and 9, respectively. The asymptotes for small and large $\hat{\xi}$ are also displayed in the respective figures. Figures 8 and 9 show that the large $\hat{\xi}$ asymptote for skin friction is reliable when $\hat{\xi} > 50$ and for temperature when $\hat{\xi} > 1000$.

When the buoyancy opposes the main stream, the negative sign in series (48) is considered. In this case the nearest singularity is located on the positive real axis at $\hat{\xi}_0 = 0.02$.

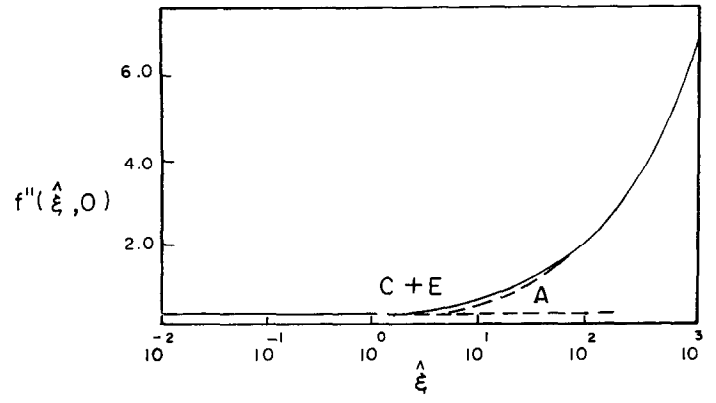

FIG. 8. Favourable case: the comparison of skin friction for mixed convection on a horizontal flat plate with constant heat flux: C+E, completed transformed series (59a); A, asymptotes for small and large values of $\hat{\xi}$.

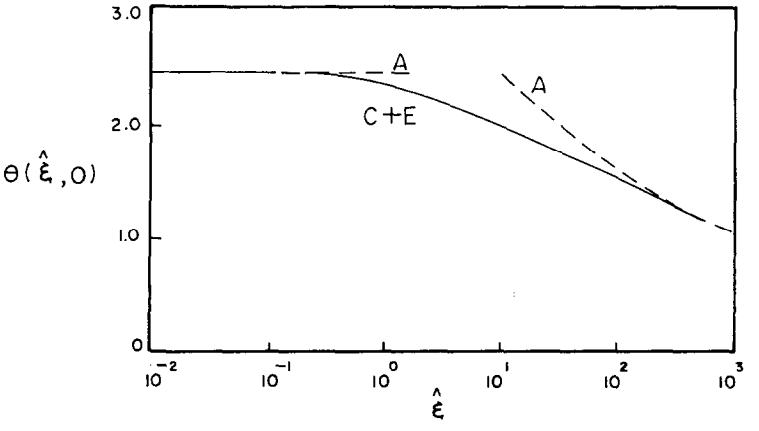

FIG. 9. Favourable case: the comparison of wall temperature for mixed convection on a horizontal flat plate: C+E, completed transformed series (59b); A, asymptotes for small and large values of $\hat{\xi}$.

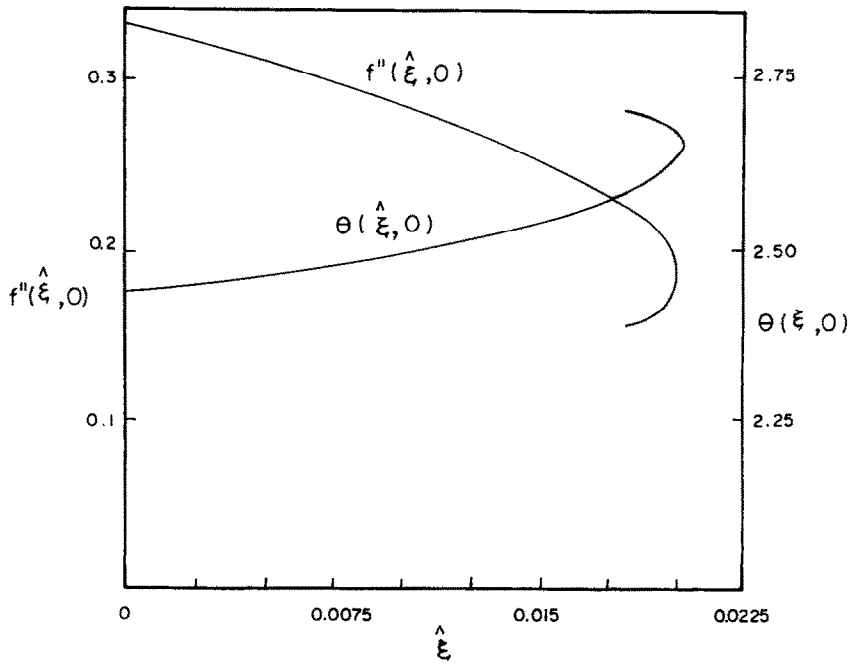

FIG. 10. Adverse case: the characteristics of mixed convection on a horizontal flat plate with constant heat flux: $F(\hat{\xi},0)$, skin friction at the wall; $\theta(\hat{\xi},0)$, temperature at the wall.

Inverting series (48) we obtain

$$\hat{\xi}(f'') = \sum_{n=1}^{9} \hat{c}_n \left(\frac{f''-a_0}{a_1}\right)^n \tag{51a}$$

$$\hat{\xi}(\theta) = \sum_{n=1}^{9} \hat{d}_n \left(\frac{\theta-b_0}{b_1}\right)^n \tag{51b}$$

where $f'' = f''(\hat{\xi},0)$, $\theta = \theta(\hat{\xi},0)$ and the coefficients $\hat{c}_n$ and $\hat{d}_n$ are given in Table 6.

The results from series (51) for skin friction and wall temperature are displayed against $\hat{\xi}$ in Fig. 10. The figure clearly shows the duality of solution and the associated turning point. The two series (51a) and (51b) give slightly different values for the turning point which may be due to the rate of convergence of the series, i.e. $\hat{\xi}_0 = 0.0203$.

Table 6. Coefficients in the inverted series (51) for skin friction and wall temperature for mixed convection on a horizontal plate with uniform heat flux

n	Skin friction $\hat{c}_n$	Wall temperature $\hat{d}_n$
1	0.100000000E+01	0.100000000E+01
2	0.997344809E+01	0.144210269E+02
3	−0.166328409E+02	0.962618465E+02
4	0.289117323E+03	0.695509689E+03
5	−0.634773406E+04	0.520628603E+03
6	0.165002917E+06	0.685086333E+05
7	−0.456090567E+07	−0.124509146E+07
8	0.143747688E+09	0.429982094E+08
9	−0.460895244E+10	−0.104170860E+10

The present results at the turning point are $\hat{\xi}_0 = 0.02$, $f''(\hat{\xi},0) = 0.18$ for $\sigma = 0.72$ whereas the corresponding values from ref. [14] are $\hat{\xi} = 0.0246$, $f''(\hat{\xi},0) = 0.1938$ for $\sigma = 1$, and $\hat{\xi} = 0.0155$, $f''(\hat{\xi},0) = 0.1515$ for $\sigma = 0.5$. Therefore, the results for the uniform heat flux case are largely in agreement with ref. [14] in the neighbourhood of the turning point.

Acknowledgement—The authors are thankful to the referee for some helpful comments.

REFERENCES

1. Y. Mori, Buoyancy effects in forced laminar convection flow over a horizontal flat plate, *J. Heat Transfer* **83**, 479–482 (1961).
2. E. M. Sparrow and W. J. Minkowycz, Buoyancy effects on horizontal boundary-layer flow and heat transfer, *Int. J. Heat Mass Transfer* **5**, 505–511 (1962).
3. E. G. Hauptmann, Laminar boundary-layer flows with small buoyancy effects, *Int. J. Heat Mass Transfer* **8**, 289–295 (1965).
4. L. G. Redekopp and A. F. Charwat, Role of buoyancy and the Boussinesq approximation in horizontal boundary layers, *J. Hydronautics* **6**, 34–39 (1972).
5. C. A. Hieber, Mixed convection above a heated horizontal surface, *Int. J. Heat Mass Transfer* **16**, 769–785 (1973).
6. L. G. Leal, Combined forced and free convection heat transfer from a horizontal flat plate, 2, *Z. Angew. Math. Phys.* **24**, 20–42 (1973).
7. O. G. Martynenko and Yu. A. Sokovishin, *Heat Transfer in Mixed Convective Flow* (in Russian). Nauka i Tekhnika, Minsk (1975).
8. T. S. Chen, E. M. Sparrow and A. Mucoglu, Mixed

convection in boundary layer flow on a horizontal plate, *J. Heat Transfer* **99**, 66–71 (1977).
9. A. Mucoglu and T. S. Chen, Mixed convection on a horizontal plate with uniform surface heat flux, *Proc. 6th Int. Heat Transfer Conf.*, Vol. I, pp. 85–90. Hemisphere, Washington, DC (1978).
10. X. A. Wang, An experimental study of mixed, forced and free convection heat transfer from a horizontal flat plate to air, *J. Heat Transfer* **104**, 139–144 (1982).
11. N. Ramachandran, B. E. Armaly and T. S. Chen, Mixed convection over a horizontal plate, *J. Heat Transfer* **105**, 420–432 (1983).
12. A. Moutsoglou, T. S. Chen and K. C. Cheng, Vortex instability of mixed convection flow over a horizontal flat plate, *J. Heat Transfer* **103**, 257–261 (1981).
13. N. K. Banthiya and N. Afzal, Mixed convection over a semi-infinite horizontal plate, *Z. Angew. Math. Phys.* **31**, 646–652 (1980).
14. W. Schneider and M. G. Wasel, Breakdown of the boundary layer approximation for mixed convection above a horizontal plate, *Int. J. Heat Mass Transfer* **28**, 2307–2313 (1985).
15. L. Pera and B. Gebhart, Natural convection boundary-layer flow over horizontal and slightly inclined surface, *Int. J. Heat Mass Transfer* **16**, 1131–1146 (1973).
16. N. Afzal, Higher order effects in natural convection flow over a uniform flux horizontal surface, *J. Thermo-Fluid Dynamics* **19**, 177–180 (1985).
17. W. Schneider, A similarity solution for combined forced and free convection flow over a horizontal plate, *Int. J. Heat Mass Transfer* **22**, 1401–1406 (1979).
18. M. S. Raju, X. Q. Liu and C. K. Law, A formulation for combined forced and free convection past horizontal and vertical surfaces, *Int. J. Heat Mass Transfer* **27**, 2215–2224 (1984).
19. N. Afzal, Mixed convection in buoyant plumes. In *Handbook of Heat and Mass Transfer Operations* (Edited by N. P. Cheremissinoff), Chap. 37. Gulf, Texas (1985).
20. N. Afzal and T. Hussain, Mixed convection over horizontal plate, *J. Heat Transfer* **66**, 240–241 (1984).
21. I. R. de Hoog, B. Laminger and R. Weiss, A numerical study of similarity solutions for combined forced and free convection, *Acta Mechanica* **51**, 139–149 (1984).
22. C. Domb and M. F. Sykes, On the susceptibility of a ferromagnetic above the Curie point, *Proc. R. Soc.* **A240**, 214–228 (1957).
23. Z. Rotem and L. Classen, Natural convection above unconfined horizontal surfaces, *J. Fluid Mech.* **39**, 173–192 (1969).
24. M. Van Dyke, Analysis and improvement of perturbation series, *Q. J. Mech. Appl. Math.* **27**, 423–450 (1974).
25. I. M. Ryshik and I. S. Gradstein, *Tables of Series, Products and Integrals*. Veb Deutscher Verlag Der Wissenschaften, Berlin (1957).
26. T. Hussain, Mixed convection on horizontal surfaces, Ph.D. thesis, Aligarh Muslim University, Aligarh, India (1985).
27. R. Narasimha and N. Afzal, Laminar boundary on a flat plate at low Prandtl number, *Int. J. Heat Mass Transfer* **14**, 279–292 (1971).

CONVECTION MIXTE A COUCHE LIMITE POUR UN ECOULEMENT UNIFORME SUR UN PLAN HORIZONTAL

Résumé—La convection mixte à couche limite sur une plaque horizontale pour un flux thermique ou une température uniforme est étudiée numériquement en utilisant une série de perturbation. Les 17 premiers termes pour le cas de température pariétale uniforme et les 10 premiers termes pour le cas du flux uniforme sont calculés pour un nombre de Prandtl $\sigma = 0{,}72$. Le développement direct est traité par la transformée d'Euler et d'autres techniques. Les résultats sont présentés pour la convection naturelle aidant ou contrariant l'écoulement principal. Pour la température pariétale, l'erreur maximale est 5,983% pour le frottement et 1,072% pour le transfert de chaleur. Pour le flux thermique uniforme, l'erreur maximale est 6,9% pour le frottement et 1,9% pour la température de paroi.

GRENZSCHICHTSTRÖMUNG IN MISCH-KONVEKTION AN EINER WAAGERECHTEN PLATTE IN EINER GLEICHFÖRMIGEN HAUPTSTRÖMUNG

Zusammenfassung—Die Grenzschichtströmung in Mischkonvektion an einer waagerechten Platte wird für die Fälle konstanter Wandtemperatur/konstanter Wärmestromdichte mit Hilfe eines erweiterten Störungsansatzes untersucht. Für eine Prandtl-Zahl $\sigma = 0{,}72$ werden bei konstanter Wandtemperatur die ersten 17 Terme, bei konstanter Wärmestromdichte die ersten 10 Terme berechnet. Die direkte Entwicklung wird mit Hilfe der Euler-Transformation und anderer Techniken transformiert. Ergebnisse für gleich- und gegengerichteten Auftrieb (bezüglich der Hauptströmung) werden vorgestellt. Die Genauigkeit ist im gesamten Strömungsgebiet zweistellig. Für konstante Wandtemperatur beträgt der maximale Fehler bei der Berechnung der Wand-Schubspannung 5,983%, beim Wärmeübergang 1,072%; für konstante Wärmestromdichte 6,9% bzw. 1,9%.

СМЕШАННОКОНВЕКТИВНЫЙ ПОГРАНИЧНЫЙ СЛОЙ НА ГОРИЗОНТАЛЬНОЙ ПЛАСТИНЕ В ОДНОРОДНОМ ПОТОКЕ

Аннотация—Смешанноконвективный пограничный слой на горизонтальной пластине для однородных температуры стенки и теплового потока исследуется разложением в ряды по возмущениям с использованием ЭВМ. Первые 17 членов для случая однородной температуры стенки и первые 10 членов для случая однородного теплового потока рассчитываются для числа Прандтля $\sigma = 0.72$. Прямое разложение в ряд проводится с помощью преобразования Эйлера и другими способами. Представлены результаты для спутного и противоположного направлений вторичного и основного течения. Результаты даны с точностью до двух значащих цифр во всей области изменения направленной вдоль потока координаты. В случае однородной температуры стенки максимальная погрешность составляла 5.983% для поверхностного трения и 1.072% для величины теплоотдачи. В случае однородного теплового потока максимальная погрешность равна 6.9% для поверхностного трения и 1.9% для температуры стенки.